

# Brevianamides with Antitubercular Potential from a Marine-Derived Isolate of *Aspergillus versicolor*

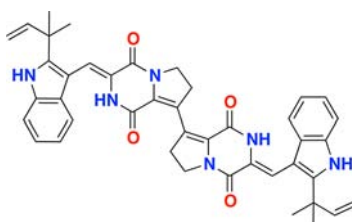
Fuhang Song,<sup>‡,†</sup> Xinru Liu,<sup>‡,†,‡,§</sup> Hui Guo,<sup>†,§</sup> Biao Ren,<sup>†,§</sup> Caixia Chen,<sup>†</sup> Andrew M. Piggott,<sup>||</sup> Ke Yu,<sup>†,§</sup> Hong Gao,<sup>†</sup> Qian Wang,<sup>†,§</sup> Mei Liu,<sup>†</sup> Xueting Liu,<sup>†</sup> Huanqin Dai,<sup>†</sup> Lixin Zhang,<sup>\*,†</sup> and Robert J. Capon<sup>\*,||</sup>

Chinese Academy of Sciences Key Laboratory of Pathogenic Microbiology and Immunology, Institute of Microbiology, Chinese Academy of Sciences, Beijing 100190, China, School of Life Sciences, University of Science and Technology of China, Hefei 230026, China, Graduate University of Chinese Academy of Sciences, Beijing 100049, China, and Division of Chemistry and Structural Biology, Institute for Molecular Bioscience, The University of Queensland, St. Lucia, Queensland 4072, Australia

zhanglixin@im.ac.cn; r.capon@uq.edu.au

Received July 25, 2012

## ABSTRACT



An *Aspergillus versicolor* isolated from sediment collected from the Bohai Sea, China, yielded the new dimeric diketopiperazine brevianamide S (1), together with three new monomeric cometabolites, brevianamides T (2), U (3), and V (4). Structures were determined by detailed spectroscopic analysis. Brevianamide S exhibited selective antibacterial activity against Bacille Calmette-Guérin (BCG), suggestive of a new mechanism of action that could inform the development of next-generation antitubercular drugs.

Tuberculosis (TB) is a leading cause of death in the world today, exacerbated by the prevalence of multidrug resistant (MDR-TB) and extreme drug resistant (XDR-TB) strains.<sup>1</sup> Despite the threat to global health, current front-line TB antibiotics are limited to a selection of vintage molecules discovered over 60 years ago [i.e., isoniazid (INH), pyrazinamide (PZA), ethambutol (EMB), rifampicin (RMP), and streptomycin (STM)], with treatments requiring protracted high dosage combination therapy.<sup>2</sup> Of great concern, MDR-TB is resistant to both

INH and RMP, while XDR-TB has additional resistance to the major second-line TB antibiotic fluoroquinolones (e.g., ciprofloxacin) and to one or more aminoglycosides (e.g., amikacin) or polypeptides (e.g., capreomycin).

A World Health Organization (WHO) report on global tuberculosis control<sup>3</sup> acknowledged 1.55–2.32 million TB deaths in 2008 and estimated that the notified cases of MDR-TB represented only 10% of real infection levels.

This report also noted that while India and China recorded the highest incidence of MDR-TB in 2007 (~131,000 and ~112,000 respectively), 57 countries had reported cases of XDR-TB by late 2009. The rapidly diminishing value of vintage antibiotics, coupled with an accelerating globalization of drug-resistant TB, represents a looming healthcare crisis that demands urgent attention. The case for investment in the discovery of new and improved TB antibiotics is compelling.

<sup>†</sup> Chinese Academy of Sciences Key Laboratory of Pathogenic Microbiology and Immunology.

<sup>‡</sup> University of Science and Technology of China.

<sup>§</sup> Graduate University of Chinese Academy of Sciences.

<sup>||</sup> The University of Queensland.

<sup>‡</sup> These authors contributed equally

(1) Lienhardt, C.; Glaziou, P.; Uplekar, M.; Loenroth, K.; Getahun, H.; Raviglione, M. *Nat. Rev. Microbiol.* **2012**, *10*, 407.

(2) Villemagne, B.; Crauste, C.; Flipo, M.; Baulard, A. R.; Deprez, B.; Willand, N. *Eur. J. Med. Chem.* **2012**, *51*, 1.

(3) Global Tuberculosis Control: A short update to the 2009 WHO Report, 2009, ISBN 978 92 4 159886 6.

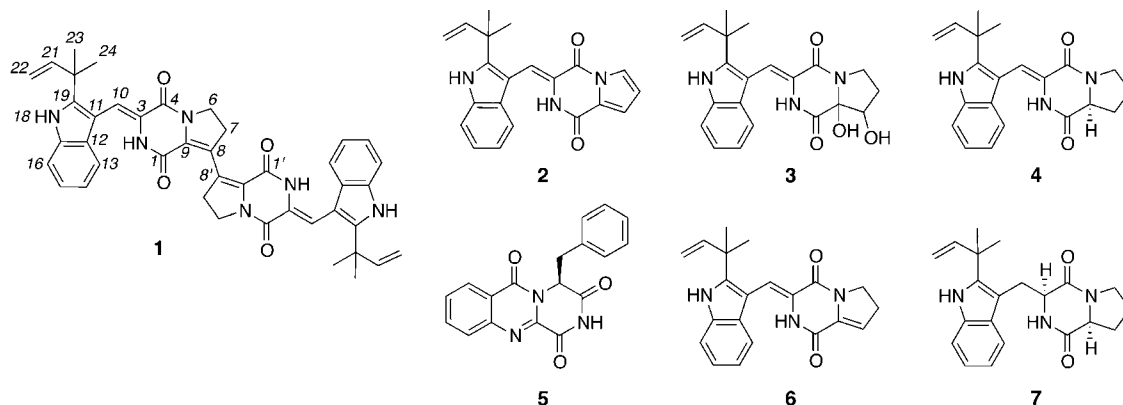


**Figure 1.** *Aspergillus versicolor* metabolites 1–7.

The historically important role played by microbial natural products in delivering modern antitubercular antibiotics is well documented.<sup>4</sup> In an effort to build on this success, we assessed a library of marine-derived bacteria (4,024) and fungi (533) for growth inhibitory activity against *Bacille Calmette-Guérin* (BCG), an attenuated strain of the bovine tuberculosis bacillus *Mycobacterium bovis*. Although BCG lacks virulence in humans, it does retain sufficient antigenicity for human vaccination purposes and also serves as a useful screening surrogate for *Mycobacterium tuberculosis*. This screening campaign detected 27 (0.6%) extracts that exhibited promising levels of anti-BCG (and potential anti-TB) activity. More specifically, an isolate of *Aspergillus versicolor* (MF030) recovered from a sediment sample collected at a depth of 60 m from the Bohai Sea, China, was prioritized for further analysis.

A large-scale culture of *Aspergillus versicolor* (MF030) comprising 12 × 1 L flasks, each charged with 100 g of rice, 3.25 g of soya bean powder, and 30 mL of artificial seawater, was incubated for 19 days, after which the combined material was extracted with EtOAc/MeOH/AcOH (80:15:5) and concentrated in vacuo to deliver a crude fraction. After solvent partitioning (H<sub>2</sub>O/EtOAc), the EtOAc solubles (13.9 g) were subjected to silica and Sephadex LH-20 chromatography, followed by reversed-phase HPLC, to yield seven diketopiperazines (DKPs) 1–7

(Figure 1). DKPs 1–4 were identified by detailed spectroscopic analysis as new members of the brevianamide class of alkaloids, brevianamides S–V (1–4).<sup>5</sup> DKPs 5–7 were identified as known members of this structural class: brevianamides N (5) and K (6),<sup>6</sup> first reported in 2009 from an undescribed isolate of *Aspergillus versicolor*, and deoxybrevianamide E (7),<sup>7</sup> first reported in 1973 from *Aspergillus ustus*. The spectroscopic analysis leading to the structure elucidation of the new metabolites 1–4 is detailed below.

HRESI(–)MS measurement on 1 detected a quasimolecular ion ([M – H]<sup>–</sup>) indicative of a molecular formula (C<sub>42</sub>H<sub>39</sub>N<sub>6</sub>O<sub>4</sub>, Δ<sub>mmu</sub> +0.8), requiring 26 double-bond equivalents (DBE). Analysis of the 1D and 2D NMR (methanol-*d*<sub>4</sub>) data for 1 (Table 1) confirmed a degree of symmetry, while consideration of the <sup>1</sup>H and 2D COSY NMR data suggested that each of the symmetric elements incorporated an *ortho*-disubstituted benzene (fragment A), an isolated sp<sup>2</sup> methine proton (fragment B), a mono-substituted olefin (fragment C), two equivalent tertiary methyls (fragment D), and an isolated XCH<sub>2</sub>CH<sub>2</sub>Y moiety (fragment E), as illustrated in Figure 2. On consideration of <sup>13</sup>C and 2D HMBC NMR data, fragments A–D could be assembled to form an indole moiety substituted as indicated by a 1,1-dimethylallyl (reverse isoprene) and a trisubstituted olefin, while fragment E was attributed to a five-membered *N*-heterocycle (Figure 2). Diagnostic HMBC and ROESY 2D NMR (pyridine-*d*<sub>5</sub>) correlations (Figure 2) positioned the amide carbonyls C-1 (δ<sub>C</sub> 156.0) and C-4 (δ<sub>C</sub> 157.5) within a linking diketopiperazine moiety, establishing a *Z* configuration about Δ<sup>3,10</sup>, accounting for all DBE and assigning a dimeric C-8 to C-8' linkage. The observations outlined above permitted assignment of the structure as indicated to brevianamide S (1).

HRESI(+ )MS measurement on 2 detected a quasimolecular ion ([M + H]<sup>+</sup>) indicative of a molecular formula (C<sub>21</sub>H<sub>19</sub>N<sub>3</sub>O<sub>2</sub>, Δ<sub>mmu</sub> +1.0) requiring 14 DBE, suggestive of an oxidized didehydro analogue of the monomeric unit

(4) (a) Salomon, C. E.; Schmidt, L. E. *Curr. Top. Med. Chem.* **2012**, *12*, 735. (b) Garcia, A.; Bocanegra-Garcia, V.; Palma-Nicolas, J. P.; Rivera, G. *Eur. J. Med. Chem.* **2012**, *49*, 1. (c) Gutierrez-Lugo, M.-T.; Bewley, C. A. *J. Med. Chem.* **2008**, *51*, 2606. (d) Copp, B. R.; Pearce, A. N. *Nat. Prod. Rep.* **2007**, *24*, 278.

(5) (a) Brevianamide S (1): orange powder; NMR (600 MHz, methanol-*d*<sub>4</sub>) see Table 1; UV (MeOH) λ<sub>max</sub> (log ε) 389 (4.21), 283 (4.29), 225 (4.61) nm; HRESI(–)MS *m/z* 691.3046 [M – H]<sup>–</sup> (calcd for C<sub>42</sub>H<sub>39</sub>N<sub>6</sub>O<sub>4</sub><sup>–</sup>, 691.3038). (b) Brevianamide T (2): light yellow powder; NMR (600 MHz, methanol-*d*<sub>4</sub>) see Table 1; UV (MeOH) λ<sub>max</sub> (log ε) 416 (3.83), 267 (3.98), 224 (4.38) nm; HRESI(+ )MS *m/z* 346.1560 [M + H]<sup>+</sup> (calcd for C<sub>21</sub>H<sub>20</sub>N<sub>3</sub>O<sub>2</sub><sup>+</sup>, 346.1550). (c) Brevianamide U (3): light yellow powder; NMR (600 MHz, methanol-*d*<sub>4</sub>) see Table 1; [α]<sub>D</sub><sup>21</sup> +20 (*c* 0.17, MeOH); UV (MeOH) λ<sub>max</sub> (log ε) 347 (3.85), 284 (3.80), 257 (3.93), 223 (4.34) nm; HRESI(–)MS *m/z* 380.1632 [M – H]<sup>–</sup> (calcd for C<sub>21</sub>H<sub>22</sub>N<sub>3</sub>O<sub>4</sub><sup>–</sup>, 380.1616). (d) Brevianamide V (4): light yellow gum; NMR (500 MHz, CDCl<sub>3</sub>) see Table 1; [α]<sub>D</sub><sup>21</sup> +39 (*c* 0.10, MeOH); UV (MeOH) λ<sub>max</sub> (log ε) 336 (4.12), 284 (4.05), 222 (4.57) nm; HRESI(+ )MS *m/z* 350.1900 [M + H]<sup>+</sup> (calcd for C<sub>21</sub>H<sub>24</sub>N<sub>3</sub>O<sub>2</sub><sup>+</sup>, 350.1863).

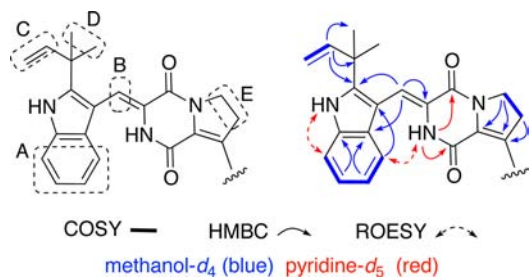
(6) Li, G.-Y.; Yang, T.; Luo, Y.-G.; Chen, X.-Z.; Fang, D.-M.; Zhang, G.-L. *Org. Lett.* **2009**, *11*, 3714.

(7) Steyn, P. S. *Tetrahedron* **1973**, *29*, 107.

**Table 1.**  $^1\text{H}$  and  $^{13}\text{C}$  NMR Data for Brevianamides S–V (1–4)

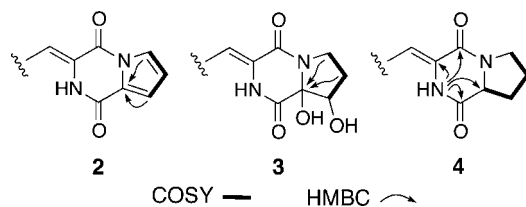
position	brevianamide S (1) <sup>a</sup>		brevianamide T (2) <sup>a</sup>		brevianamide U (3) <sup>a</sup>		brevianamide V (4) <sup>b</sup>	
	$\delta_{\text{H}}$ , mult ( <i>J</i> in Hz)	$\delta_{\text{C}}$	$\delta_{\text{H}}$ , mult ( <i>J</i> in Hz)	$\delta_{\text{C}}$	$\delta_{\text{H}}$ , mult ( <i>J</i> in Hz)	$\delta_{\text{C}}$	$\delta_{\text{H}}$ , mult ( <i>J</i> in Hz)	$\delta_{\text{C}}$
1		156.0		155.8		163.3		165.5
2							7.47, br s	
3		125.8		123.8		124.9		126.2
4		157.5		156.4		161.9		158.5
6a	4.11, dd (9.6, 9.0)	45.6	7.18, dd (3.0, 1.8)	122.2	4.07, ddd (12.0, 8.4, 8.4)	44.9	3.86, dd (12.5, 8.5)	45.9
6b					3.58, ddd (12.0, 9.6, 2.4)		3.65, dd (12.5, 10.5)	
7a	3.13, dd (9.6, 9.0)	32.5	6.66, dd (3.6, 3.0)	116.1	2.33, dddd (13.4, 9.6, 8.4, 4.2)	29.3	2.10, m	22.0
7b					1.90, ddd (13.4, 8.4, 2.4)		1.97, m	
8a		129.9	7.80, dd (3.6, 1.8)	119.2	4.41, d (4.2)	76.1	2.46, m	29.2
8b							2.04, m	
9		129.2		126.3		96.3	4.31, dd (9.5, 6.5)	59.7
10	7.18, s	113.5	7.77, s	121.3	7.35, s	116.0	7.20, s	112.8
11		104.6		105.5		104.3		103.4
12		127.2		127.0		127.3		126.2
13	7.29, ddd (7.8, 1.2, 0.6)	119.9	7.40, ddd (7.8, 1.2, 0.6)	120.2	7.24, ddd (7.8, 1.2, 0.6)	119.7	7.28, d (7.5)	119.1
14	7.04, ddd (7.8, 7.8, 1.2)	121.4	7.15, ddd (7.8, 7.8, 1.2)	122.0	7.08, ddd (7.8, 7.8, 1.2)	121.3	7.13, dd (7.5, 7.5)	121.2
15	7.13, ddd (7.8, 7.8, 1.2)	122.6	7.19, ddd (7.8, 7.8, 1.2)	123.1	7.14, ddd (7.8, 7.8, 1.2)	122.7	7.18, dd (7.5, 7.5)	122.5
16	7.43, ddd (7.8, 1.2, 0.6)	112.7	7.48, ddd (7.8, 1.2, 0.6)	113.0	7.44, ddd (7.8, 1.2, 0.6)	112.8	7.36, d (7.5)	111.5
17		136.9		137.0		136.9		134.5
18							8.36, br s	
19		146.3		148.5		146.4		144.2
20		40.5		40.7		40.5		39.4
21	6.11, dd (17.4, 10.8)	146.2	6.15, dd (17.4, 10.8)	145.9	6.11, dd (16.8, 10.8)	146.1	6.06, dd (17.0, 10.5)	144.4
22a	5.11, dd (10.8, 1.2)	112.6	5.19, dd (10.8, 1.2)	113.0	5.12, dd (10.8, 1.2)	112.7	5.22, d (10.5)	113.6
22b	5.10, dd (17.4, 1.2)		5.18, dd (17.4, 1.2)		5.10, dd (16.8, 1.2)		5.19, d (17.0)	
23	1.54, s	28.2	1.59, s	28.3	1.56, s	28.1	1.52, s	27.7
24	1.54, s	28.2	1.59, s	28.3	1.54, s	28.2	1.52, s	27.5

<sup>a</sup>  $^1\text{H}$  (600 MHz),  $^{13}\text{C}$  (150 MHz), methanol-*d*<sub>4</sub>. <sup>b</sup>  $^1\text{H}$  (500 MHz),  $^{13}\text{C}$  (125 MHz),  $\text{CDCl}_3$ .

**Figure 2.** Structure fragments and diagnostic 2D NMR correlations for brevianamide S (1).

noted above for **1**. A comparison of the NMR (methanol-*d*<sub>4</sub>) data for **2** with **1**, together with characteristic HMBC correlations, supported oxidation of the prolinyl residue in **1** to yield a trisubstituted pyrrole moiety in **2** (Figure 3). Finally, a *Z*  $\Delta^{3,10}$  configuration was tentatively attributed on biogenetic grounds, permitting the structure for brevianamide T (2) to be assigned as shown.

HRESI(–)MS measurement on **3** detected a quasimolecular ion ( $[\text{M} - \text{H}]^-$ ) indicative of a molecular formula ( $\text{C}_{21}\text{H}_{23}\text{N}_3\text{O}_4$ ,  $\Delta\text{mmu} +1.6$ ) requiring 12 DBE, suggestive of an oxidized analogue of the monomeric unit noted above

**Figure 3.** Diagnostic 2D NMR correlations for brevianamides T–V (2–4).

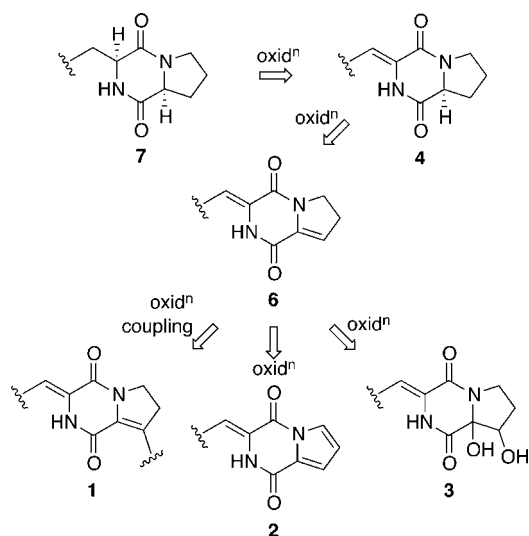
for **1**. A comparison of the NMR (methanol-*d*<sub>4</sub>) data for **3** with **1**, together with characteristic HMBC correlations, supported oxidation of the prolinyl residue in **1** to deliver a secondary OH at C-8 ( $\delta_{\text{H}}$  4.41, d, H-8;  $\delta_{\text{C}}$  76.1, C-8) and a tertiary OH at C-9 ( $\delta_{\text{C}}$  96.3, C-9) (Figure 3). As with **2**, a *Z*  $\Delta^{3,10}$  configuration was tentatively attributed to brevianamide U (**3**) on biogenetic grounds, permitting the structure to be assigned as shown. Stereochemical configurations about C-8 and C-9 remain unassigned.

HRESI(+)MS measurement on **4** detected a quasimolecular ion ( $[\text{M} + \text{H}]^+$ ) indicative of a molecular formula ( $\text{C}_{21}\text{H}_{23}\text{N}_3\text{O}_2$ ,  $\Delta\text{mmu} +2.7$ ) requiring 12 DBE, suggestive of the prolinyl precursor to the monomeric unit noted

**Table 2.** Antimicrobial Activities of 1–7

microorganism (strain)	minimum inhibitory concentration ( $\mu\text{g/mL}$ )							control
	1	2	3	4	5	6	7	
Bacille Calmette-Guérin (Pasteur 1173P2)	6.25	50	25	100	>100	50	100	0.05 <sup>a</sup>
<i>Staphylococcus aureus</i> (ATCC 6538)	>100	>100	>100	>100	>100	>100	100	1 <sup>b</sup>
<i>Bacillus subtilis</i> (ATCC 6633)	>100	>100	>100	>100	>100	>100	50	0.5 <sup>b</sup>
<i>Pseudomonas aeruginosa</i> (PAO1)	>100	>100	>100	>100	>100	>100	>100	1 <sup>c</sup>
<i>Escherichia coli</i> (ATCC 25922)	>100	>100	>100	>100	>100	>100	>100	3.12 <sup>d</sup>
<i>Candida albicans</i> (SC 5314)	>100	>100	>100	>100	>100	>100	>100	0.016 <sup>e</sup>
<i>Candida albicans</i> (SC 5314) synergistic <sup>g</sup>	>100	>100	>100	>100	>100	>100	>100	1 <sup>f</sup>

<sup>a</sup> Isoniazid. <sup>b</sup> Vancomycin. <sup>c</sup> Ciprofloxacin. <sup>d</sup> Chloramphenicol. <sup>e</sup> Ketoconazole. <sup>f</sup> Cyclosporin A. <sup>g</sup> Synergistic assay with the addition of 0.0040  $\mu\text{g/mL}$  of ketoconazole.

**Figure 4.** Plausible biosynthetic relationship between cometabolites 1–4, 6, and 7.

above for **1**. A comparison of the NMR ( $\text{CDCl}_3$ ) data for **4** with the corresponding NMR (methanol- $d_4$ ) data for **1** confirmed the absence of the  $\Delta^{8,9}$  moiety, with an L-Pro residue being confirmed by Marfey's analysis. As with **2**, a Z  $\Delta^{3,10}$  configuration was tentatively attributed to brevianamide V (**4**) on biogenetic grounds.

A plausible biosynthetic relationship linking brevianamides **1–4**, **6**, and **7** through a sequence of oxidative transformations is illustrated in Figure 4. Brevianamide S (**1**) is a new exemplar of a very rare class of dimeric diketopiperazine, of which the recently reported *Aspergillus versicolor* metabolite brevianamide J is the only other known example.<sup>6</sup>

While brevianamides **1–7** exhibited no significant antibacterial activity against the Gram-positive bacteria *Staphylococcus aureus* (ATCC 6538) and *Bacillus subtilis* (ATCC 6633), the Gram-negative bacteria *Pseudomonas aeruginosa* (PAO1) and *Escherichia coli* (ATCC 25922), or the fungus *Candida albicans* (SC 5314), the dimeric

brevianamide S (**1**) exhibited significant antibacterial activity against Bacille Calmette-Guérin (BCG). Although the potency of the anti-BCG activity attributed to **1** is modest (MIC 6.25  $\mu\text{g/mL}$ ) compared to the positive control isoniazid (MIC 0.05  $\mu\text{g/mL}$ ), the selectivity toward BCG is particularly noteworthy (Table 2).

DKPs are ubiquitous in Nature, having been isolated from bacteria, fungi, marine invertebrates, and higher organisms. Despite being known since the early 20th century, DKPs have only recently attracted significant attention for their diverse range of biological activities, including the disruption of biofilm formation through modulation of bacterial quorum sensing and their role in interkingdom cell–cell signaling.<sup>8</sup> As a first in class BCG-selective DKP dimer antibiotic, brevianamide S (**1**) is indicative of a possible new mechanism of action that could, if translated to *Mycobacterium tuberculosis*, represent a valuable new lead in the search for next-generation antitubercular drugs.

**Acknowledgment.** This work was supported in part by the National Basic Research Program of China (2012CB725200, 2012CB721006), Genzyme, a Sanofi company, the National Natural Science Foundation of China (30911120483, 81102356, 30901849, 81102369, 30973665, 30911120484), the Institute for Molecular Bioscience, The University of Queensland, and the Australian Research Council (ARC LP0989954). Part of this work was performed under research collaboration with the Global Alliance for TB Drug Development (TB Alliance) and the Institute of Microbiology of the Chinese Academy of Sciences (IMCAS). We acknowledge Z. Ma, A. Upton, and C. B. Cooper (TB Alliance) and A. Jiang (Genzyme) for their scientific input and the National Distinguished Young Scholar Program in China for an award to L.Z.

**Supporting Information Available.** Full experimental details, including microbial isolation, cultivation, and taxonomy; extraction, purification, and characterization of compounds; antimicrobial bioassays;  $^1\text{H}$  and  $^{13}\text{C}$  NMR spectra; and tabulated NMR data for all compounds. This material is available free of charge via the Internet at <http://pubs.acs.org>.

(8) de Carvalho, M. P.; Abraham, W.-R. *Curr. Med. Chem.* **2012**, *19*, 3564.

The authors declare no competing financial interest.